LASER INTERFEROMETER GRAVITATIONAL WAVE OBSERVATORY
- LIGO -
CALIFORNIA INSTITUTE OF TECHNOLOGY
MASSACHUSETTS INSTITUTE OF TECHNOLOGY

Technical Note **LIGO-T2400310-v1** 08/01/2024

2024 LIGO SURF Interim Report 2: Mapping and Correcting the Wavefront of the GQuEST End Mirrors

Erin McGee

California Institute of Technology
LIGO Project, MS 18-34
Pasadena, CA 91125
Phone (626) 395-2129
Fax (626) 304-9834
E-mail: info@ligo.caltech.edu

Massachusetts Institute of Technology
LIGO Project, Room NW17-161
Cambridge, MA 02139
Phone (617) 253-4824
Fax (617) 253-7014
E-mail: info@ligo.mit.edu

LIGO Hanford Observatory
Route 10, Mile Marker 2
Richland, WA 99352
Phone (509) 372-8106
Fax (509) 372-8137
E-mail: info@ligo.caltech.edu

LIGO Livingston Observatory
19100 LIGO Lane
Livingston, LA 70754
Phone (225) 686-3100
Fax (225) 686-7189
E-mail: info@ligo.caltech.edu

`http://www.ligo.caltech.edu/`

1 Updates and Progress

GQuEST, or Gravity from the Quantum Entanglement of Space-Time, is an experiment with the goal of measuring fluctuations in space time using an ultra-sensitive tabletop Michelson Interferometer [1]. This experiment requires high precision optics, including extremely thin high-reflectivity mirrors which will be under vacuum. This makes the optics extremely sensitive to small changes in their radius of curvature which can cause a misalignment in the modes of the light in the system. This can, in part, be mitigated by imaging the mirrors and matching the modes and by applying pressure to the mirror in a custom mount. The goal of this project is to develop a process for imaging and correcting the curvature of the mirror and analyzing how well the modes of different mirrors match.

Many of the updates and progress from the last few weeks have been centered around building the setup that we will be using to image the mirror that is similar to one that will be used in the GQuEST experiment. On the analysis side, this involves developing a way to take wavefront data that we can use to draw conclusions about the distortions in the mirror. On the experimental side, this involved cleaning and assembling the mirror mount, designing and building the setup itself, and using the setup to image using the Shack-Hartman Wavefront Sensor that we recently purchased.

1.1 Continuing research and background

A nice aspect of this project has been that there is always more to learn. In particular, since a lot of what I have been doing recently has revolved around using the Shack-Hartman Wavefront Sensor to image the wavefront of the mirror, I have been focusing on how we can use optical properties of light to analyze the wavefront. This has mostly involved looking at special functions, primarily Zernike Polynomials.

1.1.1 Shack-Hartman Wavefront Sensors

Shack-Hartman wavefront sensors are used to measure the shape of a wavefront from incident light. It consists of an array of microlenses, as can be seen in Fig. 1, usually made of fused silica, which can be either mounted or unmounted [2]. This microlens array is in front of an image sensor, like a CCD camera, which allows us to estimate the wavefront distortions from the light.

Each of the small lenses produces an intensity profile that provides information about the distortion of the wavefront coming from the optic we are imaging. By taking this intensity data and fitting Zernike coefficients to it, we can reconstruct the wavefront coming from the mirror and make statements about its curvature [3].

One disadvantage is that the resolution is limited by how many microlenses there are and how far apart they are. We found, however, that the pixel size of the CCD camera is far smaller than each spot imaged from each of the microlenes, which means we can still get good resolution from the camera.

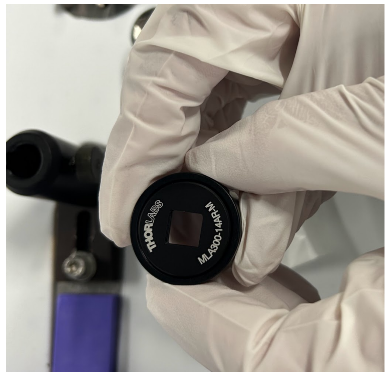

Figure 1: Microlens array in the cleanroom, before we placed it in the setup

1.1.2 Zernike Polynomials

The wavefront from the array of microlenses is reconstructed using Zernike Polynomials, since the coefficients of the wavefront can be found which by fitting the local slope of the wavefront error with Zernike polynomial derivatives. We can define the Zernike polynomial in terms of the radial distance ρ, the azimuthal angle ϕ, the integer azimuthal degree m (where $m = 0$ for spherical polynomials, and n is the radial degree. These can be seen graphed in Fig. 2, from [3], where the radial degree increases moving down the pyramid and the corresponding azimuthal degree increases going across. The corresponding function is:

$$Z_n^m(\rho, \phi) = R_n^m(\rho)\cos(m\phi) \tag{1}$$

for even polynomials and is:

$$Z_n^{-m}(\rho, \phi) = R_n^m(\rho)\sin(m\phi) \tag{2}$$

for odd polynomials. The function $R_n^m(\rho)$ is known as the radial polynomial. It can be found by using the generating function:

$$R_n^m(\rho) = \sum_{k=0}^{\frac{n-m}{2}} \frac{(-1)^k (n-k)!}{k!(\frac{n+1}{2}-k)!(\frac{n-m}{2}-k)!}\rho^{n-2k} \tag{3}$$

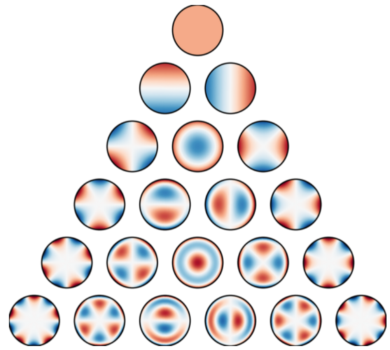

Figure 2: First 21 Zernike Polynomials

What makes Zernike polynomials a bit unique from other special functions that use integers to differentiate their modes is that we can combine the integers m and n to be known as another integer j, where:

$$j = \frac{n(n+1)+m}{2} \tag{4}$$

This means, however, that m and n are not interchangeable. In fact, $n \geq m \geq 0$. By indexing by j we can specifically recognize what kind of aberrations are present in are wavefront, as elaborated on in Section 1.5. On the microlens array itself, the shift in the lens' image is proportional to the mean slope of the wavefront on the lens. This means we can construct the wavefront (W) as a sum of the different weighted polynomials (Z) where the weight is represented by some unknown coefficient a:

$$W(\rho,\phi) = \sum_{n,m} a_{nm} Z_n^m(\rho,\phi) \tag{5}$$

Using this fact, we can reconstruct the wavefront for some set amount of Zernike polynomials. This also allows us to understand the aberrations and deformations present in the optic under analysis, which can be seen in the final column below.

Z_n^m	Z_j	Classical name
Z_0^0	1	Piston
Z_1^{-1}	$2\rho\sin\phi$	Y-tilt
Z_1^1	$2\rho\cos\phi$	X-tilt
Z_2^{-2}	$\sqrt{6}\rho^2\sin 2\phi$	oblique astigmatism
Z_2^0	$\sqrt{3}(2\rho^2-1)$	defocus
Z_2^2	$\sqrt{6}\rho^2\cos 2\phi$	vertical astigmatism

1.2 Cleaning and assembling the mirror mount

Since the mirror mount will be going under vacuum, there are certain cleaning standards that must be followed to ensure that the device does not contain any grease or dust that can effect the experiment or the equipment that it will be used with. These standards involve cleaning the mount itself as well as cleaning the tools that we will use to help us assemble the mount.

This cleaning process involves first placing the parts in a bath of a 1:30 ratio of Simple Green (an industrial grease cleaner) and deionized (DI) water. Then we sonicate the parts for about five minutes, scrub the parts, and then repeat with a bath of DI water (in order to remove the Simple Green) and a bath of isopropanol (in order to remove the water). We then and baked the custom parts from at 150°C for 48 hours. We repeated this process for both the parts to assemble the mirror mount (seen assembled in Fig. 4) and the helicoils which would act as fasteners for the screws that hold the mirror mount parts together. We then cleaned the helicoil insertion and removal tools, although these were air dried, not baked. After this, we were ready to install the helicoils into the custom parts.

Next came the assembly of the end mirror mount. First we inserted 2 mm thick silicon uncoated end mirror into the newly cleaned half ring that will hold it, as can be seen in Fig. 3. While doing this, we inserted indium foil into the joints of the rings that are holding the uncoated silicon mirror. The foil fit well when we tightened the screws, and its purpose is to be compressed by the half ring, as opposed to the mirror itself being tightened.

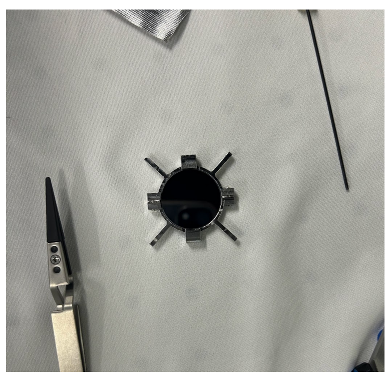

Figure 3: Uncoated Silicon Mirror in Ring Mount

After this, we assembled the rest of the front of the mirror mount. This involved adding small strips of indium foil on top of the spokes of the ring mount that goes in the center, and then screwing in the plate that covers it with vacuum safe silver screws. We held off on assembling the rest of the setup until we finished the corresponding optical setup that we would use to image the mirror. While not being assembled or used, we keep the end mirror mount wrapped in a cleanroom wipe and in aluminum foil to prevent dust and debris from getting on the mirror or the mount itself.

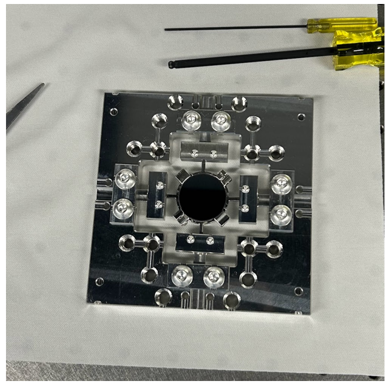

Figure 4: Uncoated Silicon Mirror in End Mirror Mount

1.3 Building the Shack-Hartman Wavefront Sensor Setup

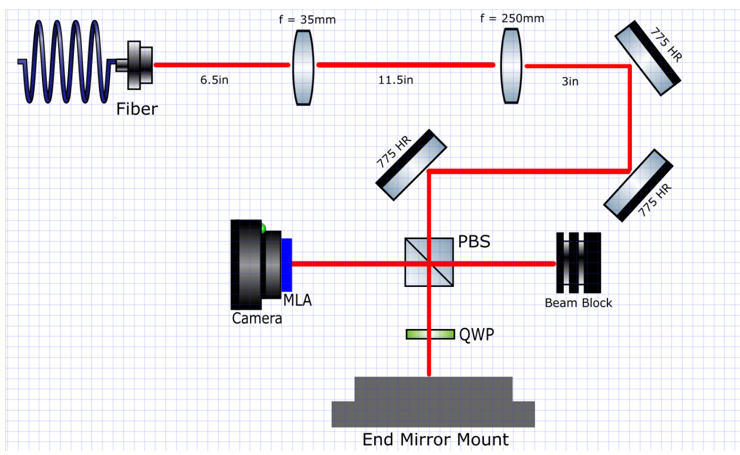

Figure 5: Setup for the Shack-Hartman Interferometer

In order to image the mirror, we have to construct an optical setup that can both fit in the lab space and that allows light to reflect off of the test mirror and then go back into the mircolens array that we purchased for this purpose, and then into the camera. This setup has had a few designs, with the most recent one being in Fig. 6 being tailored to the space we have available. To begin constructing this design, we decided to use 775nm light to image the mirror, since it would be reflected by the silicon mirror. This required us to align light from another setup into fiber coupler so we can run a 5m fiber with 775nm light from on side of the lab to the other, where we had a 1ft by 1ft area we cleared on the second table.

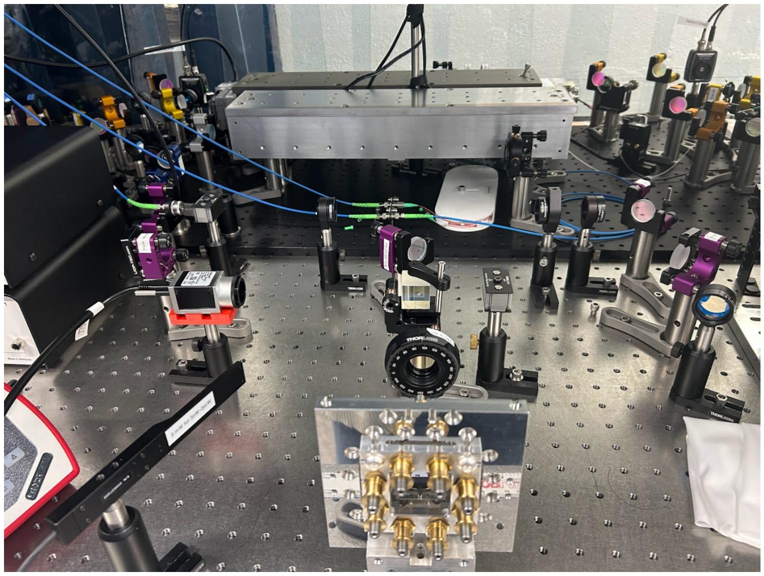

Figure 6: Setup for the Shack-Hartman Interferometer

After aligning light into and out of the fiber, we then profiled the light coming from the fiber. We found that the beam was a bit smaller than a waist than we were looking for (we want a 3mm beam waist to image as much of the mirror as possible), and decided to use a pair of lenses to diverge the beam to a larger waist and then to collimate it to remain at 3mm for the rest of the setup. We used JamMT to find a solution for this, which suggested a 35mm and a 250mm set of lenses. We aligned those and tried to re-profile the light, but we were finding that the radius of the beam was too large to use the beam profiler, and some was getting cut off. We switched to using the Basler Ace 775mm camera with an ND filter to cut down on some of the light and get a better image, and took 5 measurements, varying the camera at different points on the beam, so we could tell if the light is collimated.

To determine if the beam is actually collimated, we can see how well it matches to a Gaussian beam. This can be done by taking the parameters that make up a 2D Gaussian beam (x, y, σ_x, σ_y, etc.) and fitting them through linear regression to our data, as can be seen in Section 1.3. By comparing this fit to images taken with a CCD camera over several distances, we can measure how the beam width changes over time. As can be seen in Section 1.3, the beam width, while different in the x and y direction, is consistent across a 15in testing space.

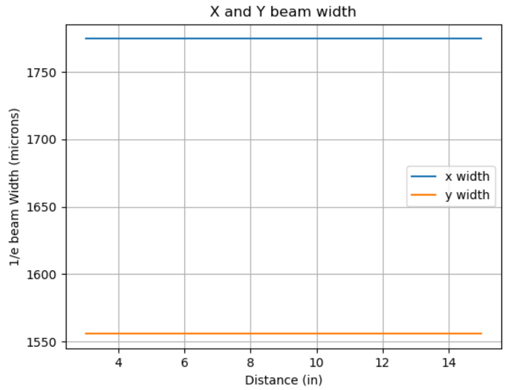

Figure 7: Change in width over 15in

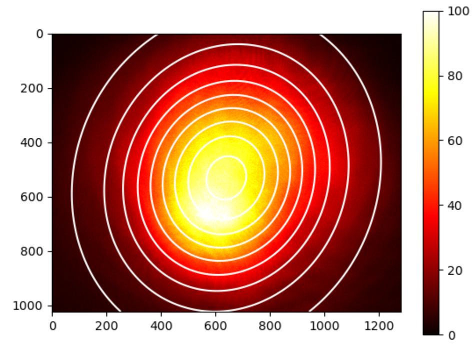

Figure 8: Gaussian fit for the beam

Finally, with the beam collimated, we were able to align the beamsplitter and the quarter wave plate (QWP). We first wanted to find a way to change the polarization of the light in the setup so that all of the light going through beamsplitter is transmitted. We could do this by rotating the fiber itself (carefully, without straining the fiber). However, this had a tendency to misalign the lenses and the mirrors when done without changing the setup, so a much better strategy was to move the beamsplitter so it is right after the fiber collimator, and then rotating the fiber until the beam fully transmits (using the power meter to make sure). Then the beamsplitter can be returned, and any final alignment can be done to the setup, including adding the quarter wave plate and the CCD camera. We also secured the microlens array in a lens tube and attached it to the CCD camera, therefore completing our setup, short of the mirror itself.

We then put in place a test mirror, which was not our full end mirror mount (see Fig. 4), but rather just a 775nm highly reflective (HR) mirror that we could test with. After a few tests, which will be discussed next, we then placed the end mirror mount in place and could begin imaging.

1.4 Imaging with the SHWS

With the Shack-Hartman setup complete, we were finally able to start imaging the wavefront of our mirror. Starting off, we imaged the 775nm HR mirror. First we added a natural density (ND) filter that cuts out about half of the light to reduce the saturation. The imaging of the microlens array can be seen in Section 1.4, where we can clearly see small areas of intensity in a grid shape. After taking this image, we added a 300mm focal length lens, which was meant to represent a curved mirror in Section 1.4. Comparing the two of these, we can see that the focuses of the microlenses change when we change the optic we are looking at. Analyzing these changes, which we will do later, is going to provide information about the curvature (which is this case we know, a good guess and check).

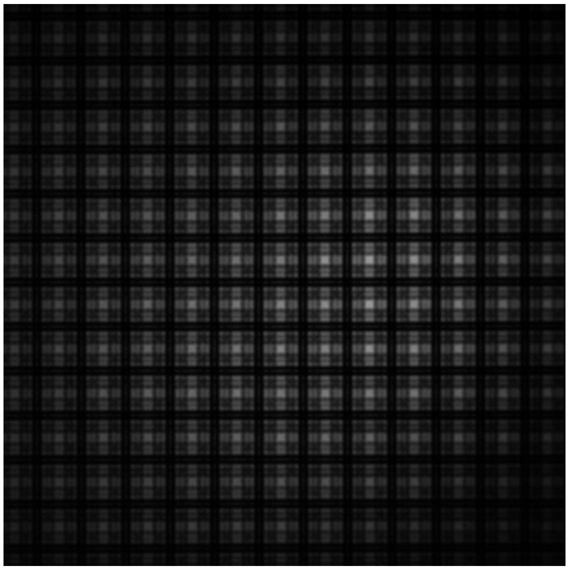

Figure 9: Imaging of a flat mirror

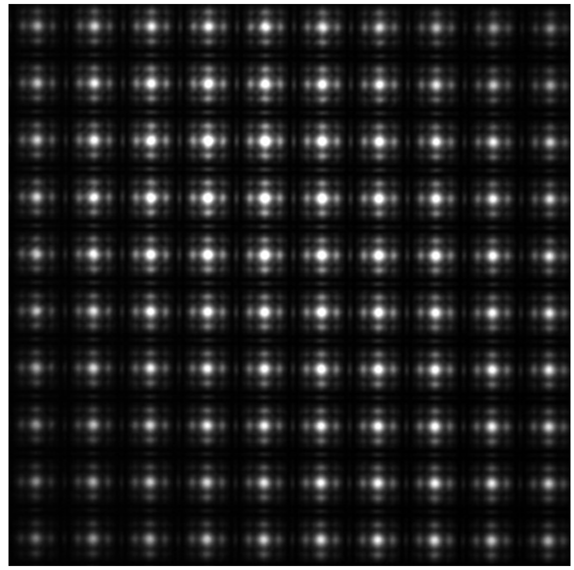

Figure 10: Imaging of a mirror with lens

After this, we removed the 775nm HR mirror and placed the end mirror mount into the same position. We then aligned the mirror into the setup, which proved to be more difficult than expected. The mirror mount is attached to a 5 axis stage, and while it does offer a lot of ways to move the mount, it did not offer a wide range of motion, which made alignment hard. Furthermore, since the silicon mirror is uncoated, it is slightly less reflective, which meant we had to turn the lights off to see the beam better.

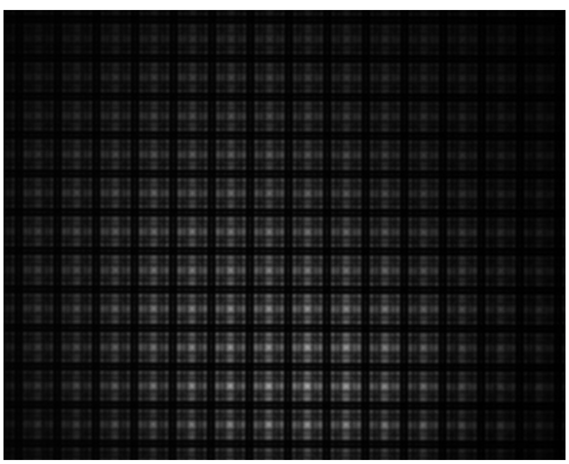

Figure 11: Uncoated mirror, MLA in front

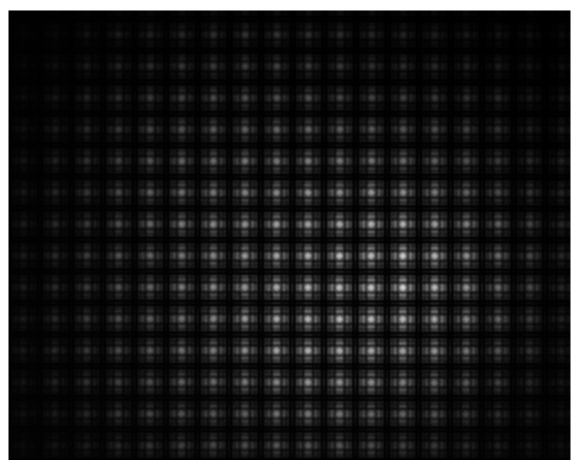

Figure 12: Uncoated mirror, MLA in back

In this round of taking images, we decided to move where in the lens tube the actual MLA is. In Section 1.4, we placed the MLA in the front of the lens tube, and therefore the aperture is closer to the beamsplitter, and in Section 1.4, it is closer to the CCD camera. This different causes a change in the microlens array (which makes sense, since we are changing where in the beam the focal length of the microlens array falls). At least for now, this means that we should take note of where exactly the microlens array is when we take data, and in the future we should try to place it in a way that maximizes the information we can get from the wavefront data.

1.5 Data Analysis

Analyzing the the Shack-Hartman data requires us to use the properties of Zernike polynomials discussed earlier in Section 1.1.2. This process is outlined by [4], which establishes a way to analyze wavefronts from phase derivative measurements like Hartman sensors, that measure local changes in the mirror distortion. This process uses a least squares estimate that relies on matrices. The first vector is P, which represents the values of the local shifts in x and y for a total number of microlenses k:

$$P = (\text{x shift 1, x shift 2, ... x shift } k\text{, y shift 1, y shift 2....y shift } k)^t \tag{6}$$

This can be thought of as the 'shifts' of each of the microlenses. It is the directional derivative of the phase, at a particular location in the microlens.

Since our P vector is the directional derivative, we need to take the derivatives of the Zernike polynomials as well in order to solve the least squares estimation and find the coefficents in Eq. (5). We can setup a matrix of our derivatives of the polynomials as:

$$D = \begin{pmatrix} \frac{\partial Z_2(x,y)_1}{\partial x} & \frac{\partial Z_2(x,y)_2}{\partial x} & \cdots & \frac{\partial Z_2(x,y)_1}{\partial y} & \cdots & \frac{\partial Z_2(x,y)_k}{\partial y} \\ \cdots & \cdots. & & \cdots & & \cdots \\ \frac{\partial Z_i(x,y)_1}{\partial x} & \frac{\partial Z_i(x,y)_2}{\partial x} & \cdots & \frac{\partial Z_i(x,y)_1}{\partial y} & \cdots & \frac{\partial Z_i(x,y)_k}{\partial y} \end{pmatrix} \tag{7}$$

Where k is the same in both matrices, meaning we can multiply P and D. The matrix we are solving for is our coefficients, A:

$$A = (a_1, a_2, a_3.....a_i) \tag{8}$$

Once we have these coefficients, we can use Eq. (5) to solve for the wavefront. Using these matrices together, we can solve the least squares expression.

$$P = D^t A$$

$$DP = DD^t A$$

$$A = (DD^t)^{-1} DP$$

Where t refers to the transpose of the matrix and -1 is the inverse. So the coefficients a_i that we need to solve for are determined by the directional derivatives of the Zernike polynomials at each of the sampling locations of the microlens.

Using this process to reconstruct the wavefront is a current work in progress, but it is the most efficient way, computationally, to determine the coefficients. Doing this is still a work in progress, but has been modeled by many others in the optics community.

2 Challenges

One of the challenges in the is project has simply been the difficulty of working with free space optics. Things that may seem small in the grand scheme of things, like getting light from one side of the lab to the other, are actually nontrivial. One small movement can misalign the entire setup, and learning how to work with free space optics has been a challenge. There are some strategies to mitigate this, though. For example, one effective strategy has been to keep notes of what the power of the beam should be at certain 'checkpoints', like coming out of the coupler, going into the beamsplitter, and before the light goes into the camera. That way, if the beam becomes misaligned, even slightly, I can simply check the power in each of the checkpoints to narrow down where the issue might be.

Another challenge has been analyzing the MLA data. The microlens array simply takes the wavefront of the mirror and changes the direction of the intensity with a very powerful lens. Therefore reconstructing the wavefront of the lens, while being essential, has been challenging to code without any loss of information.

Finally, there has been a strong challenge presented by the learning curve that is always present in doing research. This type of data analysis required to reconstruct the wavefront in particular has been difficult, since performing linear regression with such large matrices constantly runs into over flow errors and other problems that take time to solve.

3 Goals for the remainder of the project

The next steps for this project will involve using the custom end mirror mount to its full potential. As can be seen in Fig. 13, there are adjustable components of the end mirror mount that will allow us to apply a force to the mirror, changing its radius of curvature, and therefore the mode of the light in the wavefront. We want to evaluate the resolution of how much applying this force changes the modes of the light (particularly the Hermite-Gauss modes up through $n = 2$, $m = 2$).

Another goal is to re-image the mirror inside the mount in the Fizeau interferometer. While imaging with the Shack-Hartman Wavefront sensor is faster and more efficient, since we can do it in our own lab, imaging with the Fizeau interferometer is far more accurate. This will allow us to confirm our results and have a higher level of precision in this experiment.

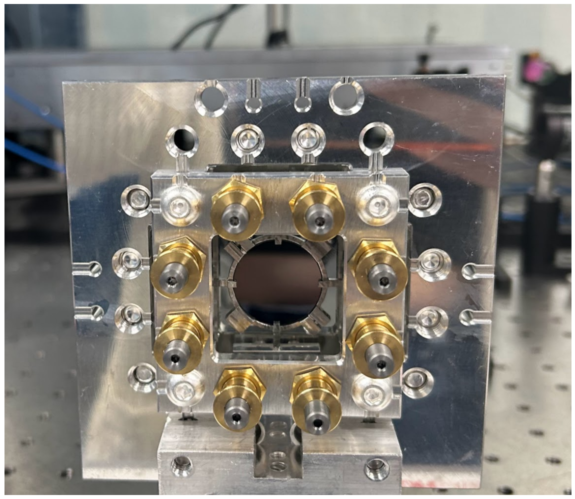

Figure 13: Adjustable components on the end mirror mount

An ongoing goal will be to continue to analyze the wavefront data that we have collected. Currently, I have written python code that I am using to analyze the data but I hope to continue to optimize and improve this analysis to streamline the process as much as possible. Since the lab focuses on precision optics, there is a strong chance that there will be another time the Shack-Hartman Wavefront sensor will be needed, so creating a streamlined process for analyzing this data will be helpful.

References

[1]S. M. Vermeulen, T. Cullen, D. Grass, I. A. O. MacMillan, A. J. Ramirez, J. Wack, B. Korzh, V. S. H. Lee, K. M. Zurek, C. Stoughton, and L. McCuller, *Photon counting interferometry to detect geontropic space-time fluctuations with gquest*, 2024.

[2]*Fused Silica Microlens Arrays — thorlabs.com*, `https://www.thorlabs.com/newgrouppage9.cfm?objectgroup_id=2861&pn=MLA300-14AR`, [Accessed 13-07-2024].

[3]*Zernike polynomials - Wikipedia — en.wikipedia.org*, `https://en.wikipedia.org/wiki/Zernike_polynomials`, [Accessed 01-08-2024].

[4]R. Cubalchini, “Modal wave-front estimation from phase derivative measurements”, J. Opt. Soc. Am. **69**, 972–977 (1979).

Acknowledgements

This work was supported by the National Science Foundation Research Experience for Undergraduates (NSF REU) program, the LIGO Laboratory Summer Undergraduate Research Fellowship program (NSF LIGO), and the California Institute of Technology Student-Faculty Programs.

This work was also supported by mentors Daniel Grass and Prof. Lee McCuller and the entire GQuEST Lab at Caltech.